Evaluation of iron-coated ZSM-5 zeolite for removal of As(III) from aqueous solutions in batch and column systems

Saeid Ezati, Bubak Souri and Afshin Maleki

ABSTRACT

Influential parameters to produce iron-coated ZSM-5 zeolite including iron loading concentration, calcination temperature and time, synthesis temperature and mixing intensity were investigated. Results showed that the optimized iron-coated ZSM-5 nano-adsorbent is produced if 40 wt.% iron loading concentration at 30 °C synthesis temperature under 60 rpm mixing intensity and 400 °C calcination temperature for 3 h are applied. Also, optimization of some parameters such as pH, adsorbent dose, contact time and temperature for removal of arsenite from aqueous solution with 400 μg/L initial concentration was considered. Evidently, the highest adsorption of arsenite occurred under pH 7, adsorbent dose 2.5 g/L, contact time 30 min and temperature 40 °C. Kinetic and isotherm models studied showed that arsenite adsorption by iron-coated ZSM-5 follows a pseudo-third-order equation and well fitted with the Langmuir isotherm model. Evaluation showed that the optimized iron-coated ZSM-5 zeolite is able to remove up to 98.37% of arsenite under the best conditions in a batch reactor. For the column system, arsenite concentration range of 0.04–97.53 μg/L in output at 1–35 min interval was confirmed and the breakthrough curve showed that iron-coated ZSM-5 nano-adsorbent was saturated after 215 min whereas Fe, pH and EC measured in output solution were 0.90 mg/L, 6.65 and 148.40 μs/cm, respectively.

Key words | As(III), aqueous solution, batch, column, iron-coated ZSM-5

Saeid Ezati
Bubak Souri (corresponding author)
Department of Environmental Sciences, Faculty of Natural Resources,
University of Kurdistan,
P.O. Box 416,
Sanandaj,
Iran
E-mail: *bsouri@uok.ac.ir*

Afshin Maleki
Environmental Health Research Center,
Kurdistan University of Medical Sciences,
Sanandaj,
Iran

INTRODUCTION

Arsenic (As) is a carcinogenic trace metal that is toxic to human and animals. It occurs naturally in soils and can be mobilized through weathering reactions and biological activities which may lead to contamination of aquifers (Mohan & Pittman 2007). Additionally, anthropogenic discharge and disposal of As-containing compounds may lead to even greater concentrations of it (Mandal & Suzuki 2002). In nature this element mainly exists as two forms of oxy-anion including arsenite As(III) and arsenate As(V) (Greenwood & Earnshaw 1997). Because of severe toxicity of As to humans its permissible concentration limit in drinking water is defined as 10 μg/l (Haque *et al.* 2008). Among the several methods that exist for removal of As, adsorption is one of the most commonly used methods (Mohan & Pittman 2007). Previous studies have demonstrated that As tends to accumulate on the surface of metal oxides such as Fe, Mn, Al, Cu, and Co residing on zeolites, pumice and clay minerals as support (Mandal & Suzuki 2002; Babaie Far *et al.* 2012). Iron oxide based materials are found effective for removal of heavy metal ions including As (arsenate and arsenite) from solutions (Sarkar *et al.* 2008). Support materials have always been considered as key factors influencing nano-adsorbent activities. Numerous micro/mesoporous materials such as zeolite (ZSM-5, clinoptilolite (Davila-Jimenez *et al.* 2008) have been applied for removal of As from aqueous solutions. Zeolite minerals such as

doi: 10.2166/ws.2016.104

ZSM-5 supports have attracted more attention due to their uniform porous structures, unique surface properties, good mechanical strength, as well as suitable chemical and hydrothermal stabilities (Tavolaro & Drioli 1999). Most of the previous researches about removal of As were conducted in batch systems only (Shih *et al.* 2015) having many shortcomings including high concentration of complicated intermediate products and long contact time (Centi *et al.* 2000), while these drawbacks might be overcome through using a fixed bed reactor (Yan *et al.* 2015). The objective of this study is to evaluate iron-coated ZSM-5 as a nano-adsorbent to remove As from aqueous solution in batch and column systems. In fact, optimization and characterization of the nano-adsorbent and the related sorption mechanisms to remove arsenite from aqueous solution is considered in a batch system while a column system is applied to assess nano-adsorbent performance and the breakthrough curve.

MATERIAL AND METHODS

Chemicals

ZSM-5 zeolite was purchased from Sigma Aldrich company (USA) while iron (III) nitrate nonahydrate ($Fe(NO_3)_3.9H_2O$) was obtained from Applychem (Germany). As stock solution As_2O_3, (1,000 $mg.L^{-1}$) was prepared by dissolving standard solution of Merck Company (Germany) in double distilled water. HCl and NaOH were used to adjust the pH of the solutions. All of the chemical reagents used in this study were analytical grade.

Iron-coated ZSM-5 zeolite

ZSM-5 zeolite was sieved through a 297 μm mesh size sieve then water washed, rinsed with double distilled water three times and dried at 85 °C for 12 h. Six samples were prepared by incipient wetness impregnation of $Fe(NO_3)_3.9H_2O$ solutions onto ZSM-5 zeolite support as iron ion concentrations were adjusted at 0, 10, 20, 30, 40, 50 and 60 wt% for iron loading onto the ZSM-5 zeolite. Next, the samples were air dried at 80 °C for 10 h and calcined in air at 400 °C for 3 h using a slow ramp of temperature (1.05 °C/min) (Yan *et al.* 2015). To study the influence of calcination temperature, the samples were calcinated in air at 200, 300, 400, 500 and 600 °C. Investigation of the influence of calcination time was achieved by conducting calcination for 2, 3, 4, 5 and 6 h. Synthesis temperature was varied from 20 °C to 70 °C by 10° increments to investigate its effect. Optimization of the mixing intensity was realized using a magnetic stirrer set up at 60, 120 and 360 rpm.

The crystallographic structures of the ZSM-5 zeolite support and iron-coated zeolite (ICZ) nano-adsorbent samples were evaluated through X-ray diffraction (XRD) patterns by an X-ray diffractometer (X'Pert MPD; Cu Kα radiation, 40 kV, 40 mA). The textural and morphological information of the samples were characterized using field emission scanning electronic microscopy (MIRA3TESCAN FE-SEM). X-ray fluorescence (XRF) analysis was carried out for elemental analysis (PW1480; Rh Kα radiation, 60 kV, 40 mA) of the samples while N_2 adsorption–desorption isotherms of catalyst sample were tested using a Micromeritics Tristar II Surface Area and Porosity (Micromeritics Instrument Co., USA) at 77.3 K.

Optimization of iron loading concentration, calcination temperature, calcination time, synthesis temperature and mixing intensity to produce optimal ICZ nano-adsorbent with the highest efficiency to adsorb arsenite from aqueous solutions was conducted in a 100 mL volumetric flask as sorption reactor, which contained 100 mg/L initial As concentration as 1.00 g of nano-adsorbent was added to the solution and the equilibrium concentration of arsenite was measured for three repeats using an atomic absorption spectrometer (Phoenix-986, Biotech Co., UK). Obtained average values were considered as the remaining arsenite concentration in the solution phase as the maximum deviation was 1.00%. The removal efficiency (*RE*) was calculated through Equation (1):

$$RE = [(C_0 - C_e/C_0)] \times 100 \quad (1)$$

whereas C_0(mg/L) and C_e(mg/L) are the initial and equilibrium concentrations of As in the solution, respectively.

Batch experiments

The batch experiments were carried out at 25 °C on a magnetic stirrer hot plate at an agitation speed of 500 rpm. 100 mL arsenite solutions with initial concentrations of

400 μg/L were added to a given amount of the ICZ in a laboratory glass reagent bottle, capped and autoclavable. Solutions of HCl and NaOH both 0.10 mol/L were used to adjust the pH. The supernatants were filtered through a 0.45 μm Whatman syringe filter to measure arsenite concentration using graphite furnace atomic absorption spectrometry. The removal efficiency, *RE*, obtained through the batch experiments was calculated using Equation (1). The amounts of arsenite sorbed at equilibrium by ICZ nano-adsorbent were calculated through Equation (2):

$$q_e = (C_0 - C_e)\frac{V}{M} \tag{2}$$

whereas q_e is the amount of adsorbed As(III) per unit mass of adsorbent at equilibrium (mg.g^{-1}), C_0 is the initial As concentration (μg/L), C_e is the equilibrium arsenite concentration in solution (μg/L), V is the volume of the As solution (L), and M is the weight of the nano-adsorbent (g) (Vergili *et al.* 2013).

Sorption kinetic

Sorption kinetics of As(III) onto ICZ nano-adsorbent were examined at various time intervals from 5 to 105 min by batch technique. 100 mL solution of arsenite of known concentration and optimal adsorbent dose was taken in airtight 150 mL conical flasks. Sorption kinetics was studied in arsenite solution with an initial concentration of 400 μg/L under an optimized temperature, pH and reacted adsorbent dose of ICZ nano-adsorbent, as contact time varied from 5 to 105 min. Pseudo-first-order (PS1), pseudo-second-order (PS2) and pseudo-third-order (PS3) models were applied to find out the adsorption mechanism. The PS1, PS2 and PS3 models are given in Equations (3)–(5) (Ho 2006; Zhou *et al.* 2009):

$$\ln [A]_t = -k_1 t + \ln [A]_0 \tag{3}$$

$$\frac{1}{[A]_t} = K_2 t + \frac{1}{[A]_0} \tag{4}$$

$$\frac{1}{[A]_t^2} = k_3 t + \frac{1}{[A]_0^2} \tag{5}$$

whereas $[A]_0$ and $[A]$ are initial concentration and momentary concentration (mol/L), respectively, while t is the time (min). k_1, k_2 and k_3 are rate constants for the pseudo-first-order (1/min), pseudo-second-order (L/mol.min) and pseudo-third-order adsorptions (L^2/mol^2.min) respectively.

Sorption isotherm

Sorption isotherms were investigated by varying amounts of adsorbents ranging from 0.5 to 2.5 g/L at a constant initial As(III) concentration of 400 μg/L under pH = 7 for 30 min contact time using Freundlich and Langmuir models (Jeong *et al.* 2007; Samarghandi *et al.* 2009). The basic assumption of the Langmuir isotherm is that adsorption happens at specific homogeneous sites which form a monolayer on the sorbent surface. The Langmuir model is given by Equation (6):

$$q_e = \frac{q_m b C_e}{1 + bC_e} \tag{6}$$

whereas q_m represents the maximum amount of adsorbed arsenite per unit mass of sorbent (mg/g), b is the Langmuir constant (1/mg), related to the energy of adsorption and increases with the increasing adsorption bond strength and C_e indicates the equilibrium concentration. The experimental Freundlich model is based on sorption at the heterogeneous surface and is given by Equation (7):

$$q_e = K_f C_e^{1/n} \tag{7}$$

whereas K_f is the Freundlich constant (mg/g)(mg/L)$^{-1/n}$, indicative of the relative adsorption capacity of adsorbent and the constant n is the Freundlich equation exponent.

Column experiments

The column tests were carried out with a double glazing glass column of 60 cm height, 0.5 cm inner and 2 cm outside diameter. The external wall was made to adjust the temperature of the column by a mini water pump and a hot plate. The column's internal wall was packed with 4 g of granular ICZ nano-adsorbent having a mesh size ranging from 18 to 10. Both sides of the column, to prevent exhaustion of the nano-adsorbent into solution, were blocked by syringe filter.

For this study, the column was used as a fixed-bed up-flow reactor; influent water was pumped through the column with a peristaltic pump. The sorption column was fed with 279 mL.h^{-1} flow rate as 1,000 mL arsenite solution with initial concentration of 400 μg/L was used. Optimal temperature and air-free tap water (without arsenite) ran through the column for 24 h before starting the experiments in order to wet the column and equilibrium establishment between the adsorbent and the water.

RESULTS AND DISCUSSION

ICZ optimization

Influence of iron loading concentration

Iron ions concentrations were adjusted to obtain 0 (pure ZSM-5), 10, 20, 30, 40, 50 and 60 wt.% of iron loading onto the ZSM-5 zeolite. The experimental results depicted in Figure 1 indicated that when iron concentration is low; the majority of the zeolite surface is not involved in adsorption of arsenite. Oppositely, when iron concentration is high; ZSM-5 zeolite surface is almost blocked and agglomeration of iron nano-particles occurs (Yan *et al.* 2015) and this can decrease removal of arsenite in high concentrations of iron ions. According to the results of this study ICZ with 40% of iron concentration is the optimal nano-adsorbent which is able to adsorb up to 74.10% of arsenite from aqueous solution.

Influence of calcination temperature

Calcination temperature has an important influence on activity of the catalysts (Zazo *et al.* 2009). Hence, various calcination temperatures including 200, 300, 400, 500 and 600 °C were tested and the results are presented in Figure 2.

Evidently, ICZ produced using 400 °C as optimal calcination temperature is able to remove up to 74.81% of arsenite from aqueous solution. Application of calcination temperatures either more or less than 400 °C may reduce the active surface of ICZ due to agglomeration of iron nano-particles over ZSM-5 zeolite and the declination effect on the porous structure, respectively (Zazo *et al.* 2009).

Influence of calcination time

The crystallization process requires a specific amount of time to be completed. Investigation of optimal calcination time to produce ICZ was conducted through application of various calcination times including 2, 3, 4, 5 and 6 h. The results proved that 3 h calcination time has the highest efficiency, producing an ICZ which can remove up to 74.30% of arsenite from aqueous solution (Figure 3). Crystallization is a process that needs time. Thereupon in less than 3 h crystallization phase formation will be incomplete. Also

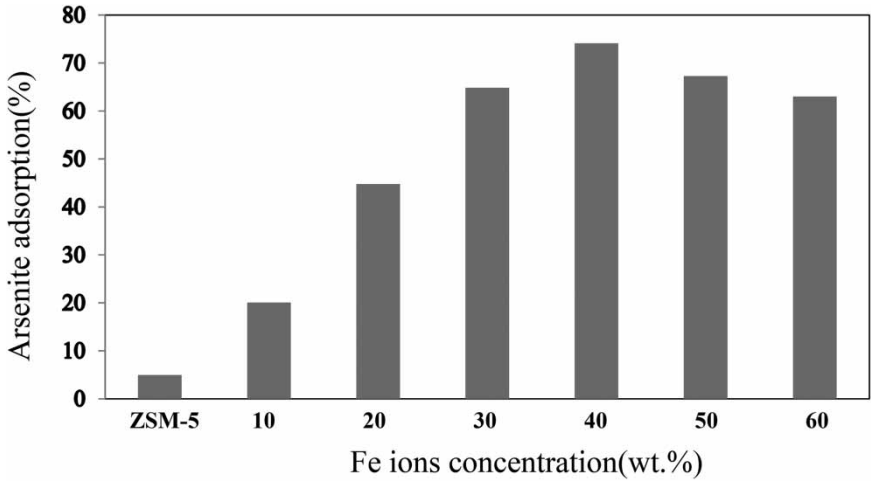

Figure 1 | Influence of Fe loading concentration on arsenite adsorption by ICZ (calcination temperature = 400 °C, calcination time = 3 h, synthesis temperature = 30 °C and mixing intensity = 60 rpm).

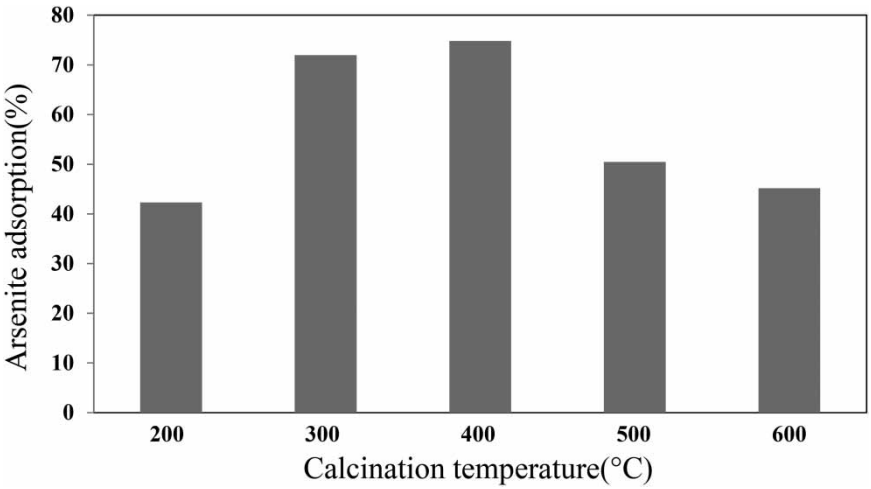

Figure 2 | Influence of calcination temperature on arsenite adsorption by ICZ (Fe concentration = 40%, calcination time = 3 h, synthesis temperature = 30 °C and mixing intensity = 60 rpm).

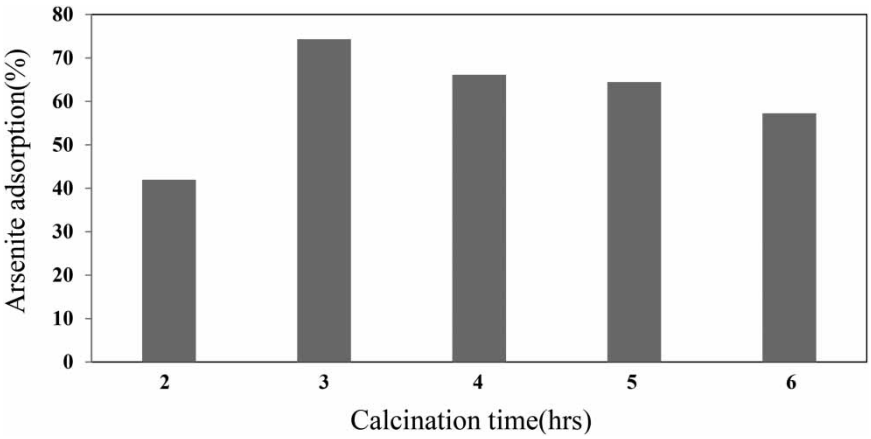

Figure 3 | Influence of calcination time on arsenite adsorption by ICZ (Fe concentration = 40%, calcination temperature = 400 °C, synthesis temperature = 30 °C and mixing intensity = 60 rpm).

in more than 3 h due to excessive growth of crystals of the active phase, surface to volume ratio dropped and thus because of the inaccessibility of a sufficiently high level, analyte adsorption rate will be reduced (Jones 2002).

Influence of synthesis temperature

Elemental adsorption on an adsorbent can be affected by ambient temperature (Vergili *et al.* 2013). In this study, iron and ZSM-5 zeolite are the adsorbate and adsorbent, respectively, whereas 20, 30, 40, 50, 60 and 70 °C were applied to investigate optimal synthesis temperature. The results showed that the best efficiency is expected for the ICZ synthesized under 30 °C temperature which could remove up to 73.23% of arsenite (Figure 4). Since the adsorption reaction is an exothermic process, application of high temperature for iron coating on the zeolite was ineffective while the coating process decreases significantly under low temperature due to decreasing molecular movement.

Influence of mixing intensity

Mixing intensity can strongly affect the reaction processes going on in a solution environment (Maiti *et al.* 2007). Therefore, coating iron on the zeolite can be affected by this parameter. It seems that low mixing intensity improves

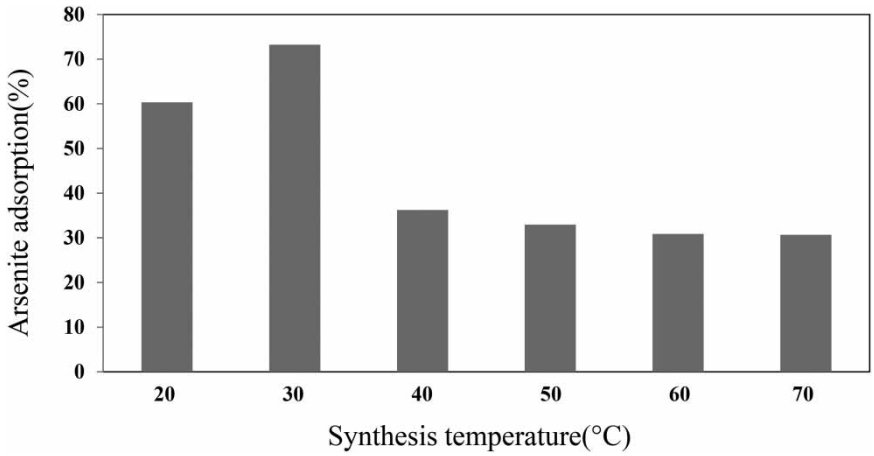

Figure 4 | Influence of synthesis temperature on arsenite adsorption by ICZ (Fe concentration = 40%, calcination temperature = 400 °C, calcination time = 3 h and mixing intensity = 60 rpm).

arsenite removal by ICZ as 60 rpm had the best efficiency among 60, 120 and 360 rpm stirring rates, having an efficiency of 75.41% (Figure 5). Adjusting stirring rate at high speed makes it difficult for iron to efficiently coat the zeolite.

ICZ characterization

XRD

Crystallographic structures of the ZSM-5 zeolite support and ICZ nano-adsorbent samples were studied by XRD as shown in Figure 6. The resulting XRD patterns represent the diffraction peaks at $2\theta = 23–25^\circ$ matching well with the standard phase of ZSM-5 zeolite (Treacy & Higgins 1996). For the ICZ sample, some peaks of iron oxide are detected. The diffraction peaks of ZSM-5 zeolite cannot be clearly detected when iron was coated on the zeolite, which could be related to agglomeration and high concentration of Fe_2O_3 component wrapping the ZSM-5 zeolite support.

FE-SEM

Illustrated in Figure 7, morphology of ZSM-5 zeolite support and optimized ICZ nano-adsorbent were compared using

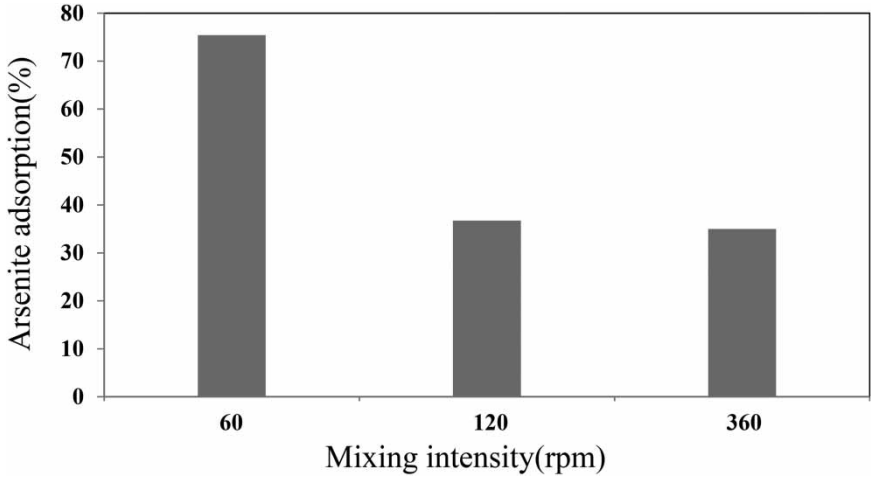

Figure 5 | Influence of mixing intensity on arsenite adsorption by ICZ (Fe concentration = 40%, calcination temperature = 400 °C, calcination time = 3 h and synthesis temperature = 30 °C).

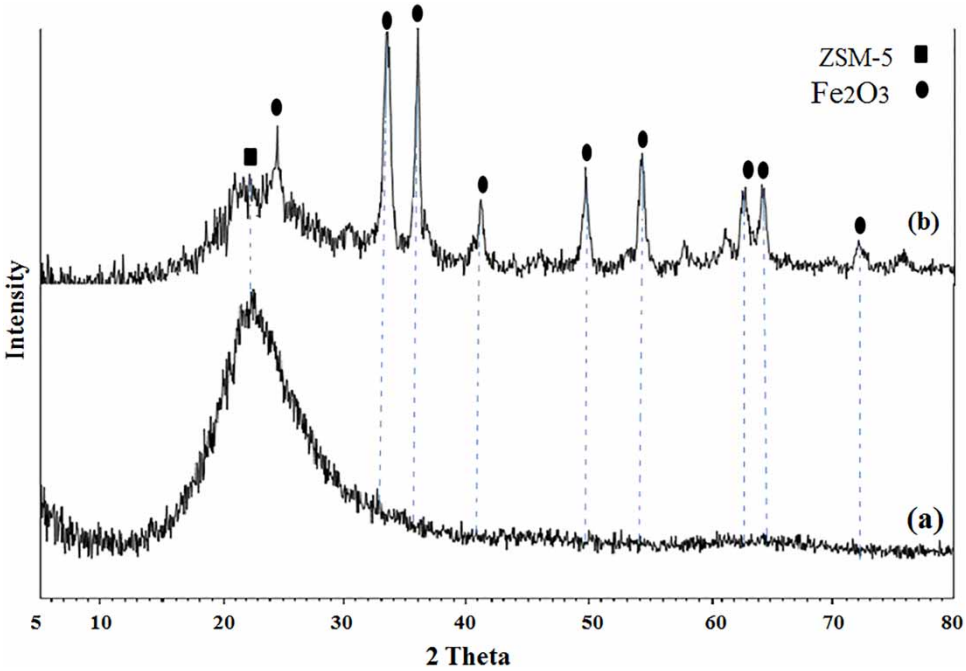

Figure 6 | XRD patterns of the samples. (a) ZSM-5 zeolite support. (b) Optimized ICZ.

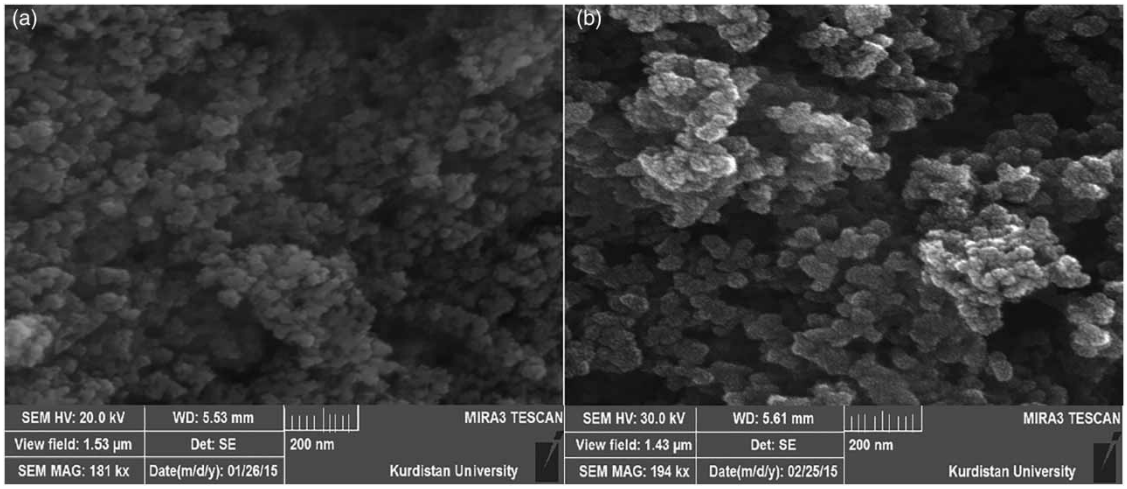

Figure 7 | FE-SEM images of the support and nano-adsorbent samples. (a) ZSM-5 zeolite support. (b) Optimized ICZ.

Table 1 | Average chemical composition of ZSM-5 zeolite and ICZ

	Content (wt%)							
	SiO_2	Al_2O_3	Fe_2O_3	CaO	MgO	K_2O	Na_2O	LOI[a]
ZSM-5	88.75	0.77	0.35	0.03	0.00	0.01	0.28	9.61
ICZ	58.26	0.32	34.19	0.03	0.00	0.01	0.12	6.93

[a]Loss on ignition.

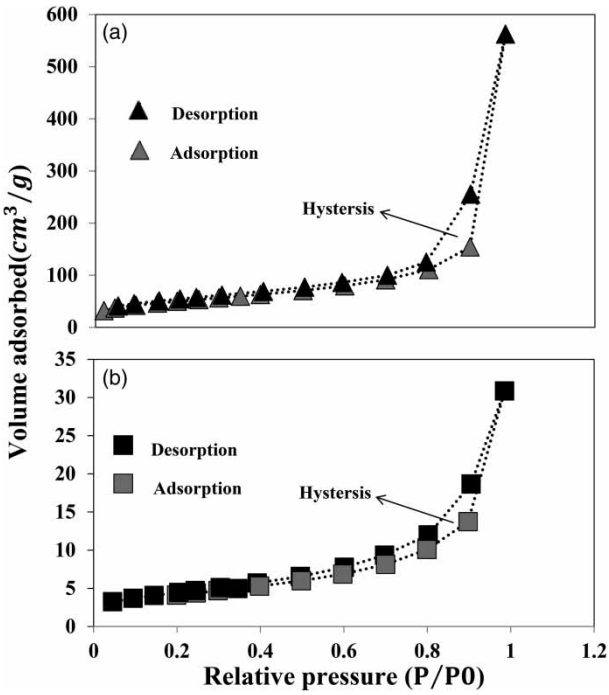

Figure 8 | N_2 adsorption–desorption isotherms of the samples at 77.3K. (a) ZSM-5 zeolite support. (b) ICZ.

Table 2 | Physiochemical properties of the samples

Sample	$V_{Micro\text{-}Pore}$ (cm^3/g)	$S_{Micro\text{-}Pore}$ (m^2/g)	S_{BET} (m^2/g)
ZSM-5 zeolite	0.09	29.51	191.70
ICZ	0.01	0.89	16.68

FE-SEM (Yan *et al.* 2015), which proved that Fe_2O_3 particles were loaded and well distributed on surface of the ZSM-5 zeolite. The results indicated that following the coating process, Fe_2O_3 particles wrapped the zeolite particles like a blanket as the mean size of the particles for ZSM-5 zeolite and optimized ICZ were 18.43 and 32.58 nm, respectively.

XRF

Results of the elemental analysis by XRF for ZSM-5 and ICZ are shown in Table 1. It appears that SiO_2, Al_2O_3 and Fe_2O_3 are the major components (Chareonpanich *et al.* 2004) as Si/Al and Si/Fe molar ratios measured were 98.35 and 343.86 for the ZSM-5 zeolite and 154.00 and 3.32 for optimized ICZ, respectively.

Specific surface area and porosity properties of ZSM-5 zeolite support and granular ready-to use ICZ were determined by N_2 adsorption–desorption (Yan *et al.* 2015). Figure 8 shows N_2 adsorption–desorption isotherms of the samples and Table 2 contains the related BET surface area and pore properties. Evidently, the volume of N_2 adsorbed increases with increasing relative pressures for all of isotherms, due to the filling of micropores in the ZSM-5 zeolite support and granular ICZ nano-adsorbent. The volume of N_2 adsorbed increases continually when the relative pressures increase, which may happen following

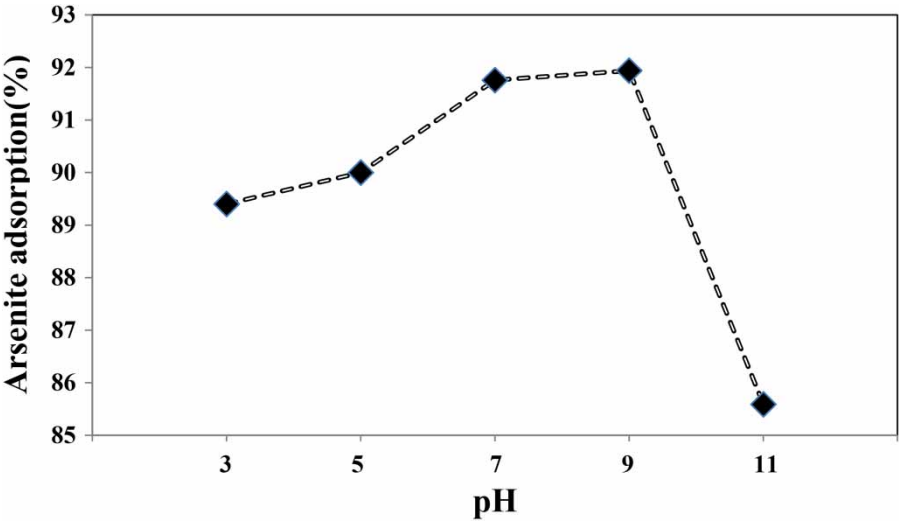

Figure 9 | Effect the change of pH on arsenite adsorption using ICZ (adsorbent dose = 10 g/L, temperature = 25 °C, initial concentration = 400 μg/L, contact time = 60 min and mixing intensity = 500 rpm).

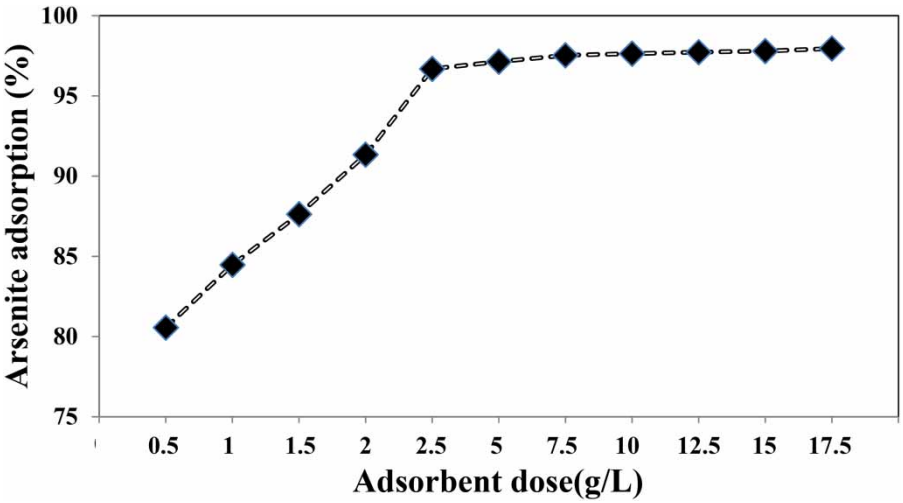

Figure 10 | Effect of adsorbent dose on arsenite adsorption using ICZ (pH = 7, temperature = 25 °C, initial concentration = 400 μg/L, contact time = 60 min and mixing intensity = 500 rpm).

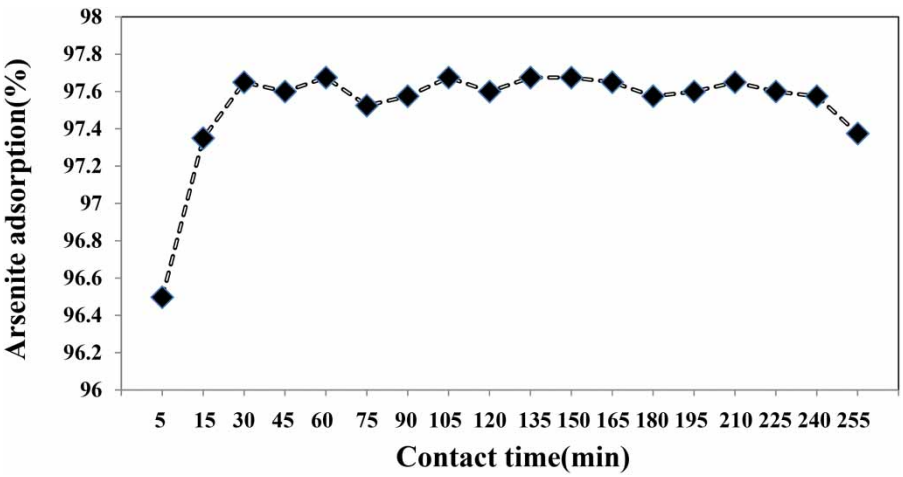

Figure 11 | Effect of contact time on arsenite adsorption using ICZ (pH = 7, temperature = 25 °C, initial concentration = 400 μg/L, adsorbent dose = 2.5 g/L and mixing intensity = 500 rpm).

multilayer adsorption of N_2. The hysteresis phenomenon demonstrated in Figure 8 proved the existence of mesopores in both ZSM-5 zeolite and granular ICZ.

Batch experiments

pH

Percentage of As (III) removed by ICZ was about 89–92% in a pH range of 3.0–9.0 from the As solution having an initial concentration of 400 μg/L. As Figure 9 shows, As percentage

Table 3 | Isotherm constants for As(III) adsorption using ICZ

Isotherm models	Content
Langmuir	
q_m (mg/g)	0.00
b (1/mg)	48.87
R^2	0.99
Freundlich	
K_f (mg/g)(mg/L)$^{-1/n}$	0.00
n	2.88
R^2	0.97

removal decreased rapidly with further increase in pH. Ferric iron in aqueous solutions in accordance with pH value produces $FeOH^{+2}$, $Fe(OH)_2^+$, $Fe(OH)_3^0$ and $Fe(OH)_4^-$ species (Katsoyiannis & Zouboulis 2002). In pH < 9.0 arsenite existed as H_3AsO_3 species (Smedley & Kinniburgh 2001) whereas in pH > 9.0 it is available as a no-valence species of arsenite. In pH = 5 to 7 ferric iron produces Fe $(OH)_2^+$ and but in pH = 7 to 9, $Fe(OH)_3^0$ is mostly produced. Therefore, change of pH through increasing OH^- ions does not appear to have significant influence on arsenite adsorption on the ICZ nano-adsorbent in pH = 5 to 9. However, ferric iron produces Fe $(OH)_4^-$, while dominant forms of arsenite are $H_2AsO_3^-$, $HAsO_3^{2-}$ and AsO_3^{3-} at pH > 9.0. Hence, a decrease in arsenite adsorption is reasonable due to electrostatic repulsion between ICZ nano-adsorbent surface and arsenite anions in pH > 9 (Maiti *et al.* 2007). As(III) adsorption on ICZ was almost pH dependent at pH = 5 to 9, which economically justifies application of ICZ for removal of arsenite in natural water pH (6.5–9). In this study, pH = 7 was found optimum for arsenite adsorption using ICZ from aqueous solution.

Adsorbent dose

The effect of adsorbent dose on percentage removal of As(III) is illustrated in Figure 10, which reveals that uptake of As(III) increases rapidly from 0.5 to 2.5 g/L but marginally thereafter. The initial increase in the efficiency of removal may be attributed to the fact that more surface area is available for arsenite to be adsorbed with increase in adsorbent dose. Further increment of adsorbent dose to more than 2.5 g/L does not seem efficient due to non-availability of adsorbate.

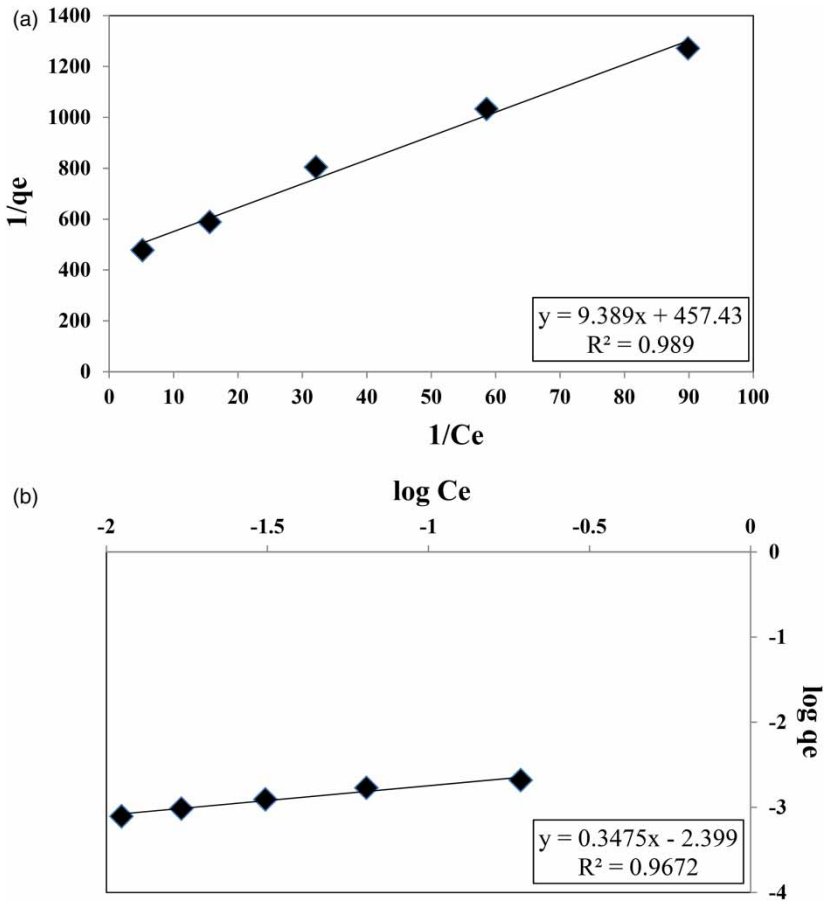

Figure 12 | Isotherm plots for As(III) adsorption on ICZ. (a) Langmuir isotherm. (b) Freundlich isotherm (pH = 7, initial concentration = 400 μg/L, temperature = 40 °C, contact time = 30 min and mixing intensity = 500 rpm).

Contact time

Contact time influence for arsenite adsorption on ICZ was tested using various time intervals between 5 and 255 min. The results showed that adsorption rates of As(III) were high at the beginning of the tests but declined gradually (Figure 11). In fact, the amount of adsorbed As(III) remained nearly unchanged after 30 min, indicating equilibrium conditions, which suggested the optimum contact time for arsenite

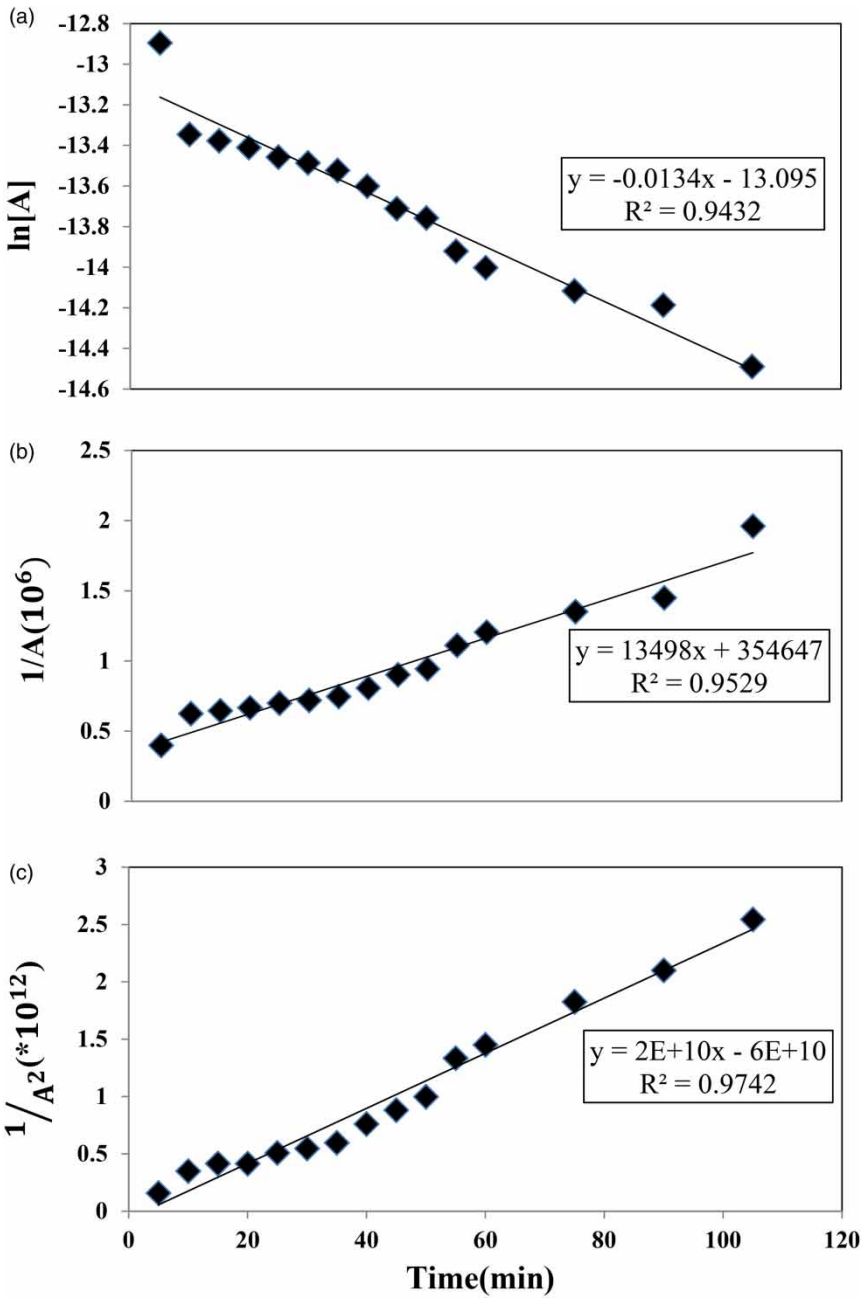

Figure 13 | Kinetic plots for As(III) adsorption on ICZ. (a) PS1. (b) PS2. (c) PS3 (pH = 7, initial concentration = 400 μg/L, temperature = 40 °C and mixing intensity = 500 rpm).

Table 4 | Parameters of kinetic models for As(III) adsorption on ICZ

Kinetic models	Content
PS1	
$k_1(1/\text{min})$	0.0134
R^2	0.94
PS2	
$k_2(L/\text{mol.min})$	13,498
R^2	0.95
PS3	
$k_3(L^2/\text{mol}^2.\text{min})$	1,024
R^2	0.97

adsorption by ICZ. Changes in arsenite adsorption between 5 and 30 min were negligible indicating one of the attractions of ICZ nano-adsorbent.

Sorption isotherm

According to Table 3 and Figure 12, it is evident from the R^2 value of the results that the Langmuir adsorption isotherm can better describe the type of reactions conducted in this study.

Sorption kinetic

Results for investigation of the kinetic models are shown in Figure 13 and PS1, PS2 and PS3 constants accompanied by R^2 are represented in Table 4. Comparing the obtained R^2 values revealed that the PS3 model is more appropriate to describe the studied adsorption process.

Column experiments

For modeling the adsorption process in a fixed bed column, column dynamic behavior is described by the breakthrough curve (Chu 2004). The breakthrough curve shows loading of the ion in the solution over the substrate of adsorbent in a column, where change concentration of adsorbed ions (C_e–C_0) or normalized output concentration (C_e/C_0), is expressed as a function of time or output volume (Aksu & Gonen 2004). The adsorption column was operated until no further arsenite removal was observed. Breakthrough curves obtained during this study are depicted in Figure 14, which shows that arsenite removal is initially high but decreases progressively over time in the column. Also in the output solution, As, Fe, pH and EC were measured. The results proved that arsenite solution in output at 1–35 min intervals was 0.04–97.53 μg/L, which suggests that in this period of time, arsenite can be removed significantly. Also, results of investigating the breakthrough curve showed that Fe-ZSM-5 nano-adsorbent was saturated after 215 min, whereas values of Fe, pH and EC measured were 0.90 mg/L, 6.65 and 148.40 μs/cm, respectively.

CONCLUSIONS

According to the results, synthesis of optimized ICZ nano-adsorbents is expected when 40 wt.% of iron loading

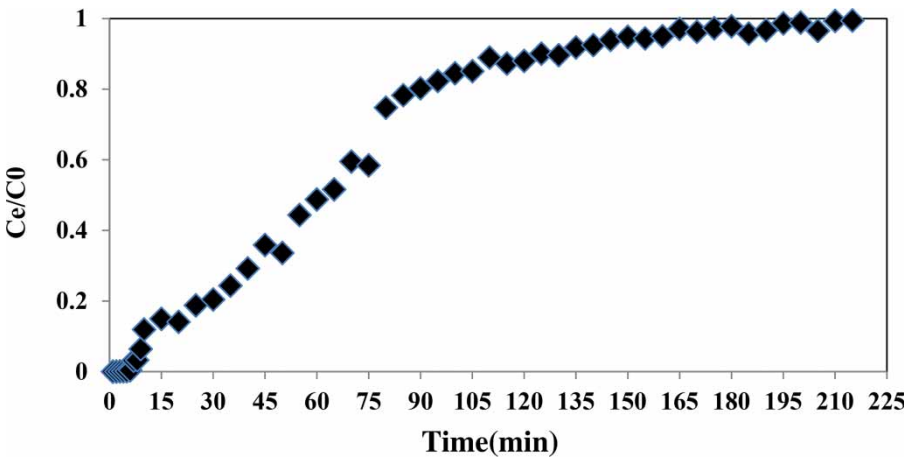

Figure 14 | Breakthrough curve in ICZ for As(III) adsorption (initial concentration = 400 μg/L, temperature = 40 °C volume of solution = 1 L and flow rate = 279 mL.h^{-1}).

concentration at 30 °C synthesis temperature under 60 rpm mixing intensity and a 400 °C calcination temperature for 3 h is applied. Evaluation of the optimized ICZ confirmed that the highest efficiency of arsenite removal happens for pH = 7, adsorbent dose = 2.5 g/L, contact time = 30 min and temperature = 313 K (40 °C). Moreover, ICZ nano-adsorbent under optimal conditions can remove 98.37% of arsenite with 400 μg/L initial concentration from aqueous solution for the batch system. For the column system, the range of arsenite concentration in the output at 1–35 min intervals was 0.04–97.53 μg/L, which suggests significant arsenite removal in this period of time as a better performance is expected through application of slower flow and/or smaller granules of nano-adsorbent for practical uses. Moreover, the results of investigation of the breakthrough curve showed that Fe-ZSM-5 nano-adsorbent was saturated after 215 min; Fe, pH and EC measured in output were 0.90 mg/L, 6.65 and 148.40 μs/cm, respectively.

ACKNOWLEDGEMENTS

The authors appreciate valuable advice from Mr Rohollah Ezati from the University of Razi (Kermanshah/Iran) and Ms Leila Babaie Far from the University of Kurdistan (Sanandaj/Iran) during the experimental stages of the study. Help from Dr Saeid Dehestani Athar, Kurdistan University of Medical Sciences (Sanandaj/Iran), is also acknowledged for his advice on the applied peristaltic pump used during the column test.

REFERENCES

Aksu, Z. & Gonen, F. 2004 Biosorption of phenol by immobilized activated sludge in a continuous packed bed: prediction of breakthrough curves. *Process Biochemistry* **39** (5), 599–613.

Babaie Far, L., Souri, B., Heidari, M. & Khoshnavazi, R. 2012 Evaluation of iron and manganese-coated pumice application for the removal of As(v) from aqueous solutions. *Iranian Journal of Environmental Health Science & Engineering* **9** (12), 9–21.

Centi, G., Perathoner, S., Torre, T. & Verduna, M. G. 2000 Catalytic wet oxidation with H_2O_2 of carboxylic acids on homogeneous and heterogeneous Fenton-type catalysts. *Catalyst Today* **55** (1–2), 61–69.

Chareonpanich, M., Namto, T., Kongkachuichay, P. & Limtrakul, J. 2004 Synthesis of ZSM-5 zeolite from lignite fly ash and rice husk ash. *Fuel Processing Technology* **85** (15), 1623–1634.

Chu, K. H. 2004 Improved fixed-bed models for metal biosorption. *Chemical Engineering Journal* **97** (2–3), 233–239.

Davila-Jimenez, M. M., Elizalde-Gonzalez, M. P., Mattusch, J., Morgenstern, P. & Perez-Cruz, M. A. 2008 In situ and *ex situ* study of the enhanced modification with iron of clinoptilolite-rich zeolitic tuff for arsenic sorption from aqueous solutions. *Journal of Colloid and Interface Science* **322** (2), 527–536.

Greenwood, N. N. & Earnshaw, A. 1997 Chemistry of elements. 2nd edn, Pergamon Press, Oxford, Boston, UK, p. 1341.

Haque, N., Morrison, G., Aguilera, I. C. & Torresdey, J. L. G. 2008 Iron-modified light expanded clay aggregates for the removal of arsenic (V) from groundwater. *Microchem. Journal* **88** (1), 7–13.

Ho, Y. S. 2006 Second-order kinetic model for the sorption of cadmium onto tree fern: a comparison of linear and non-linear methods. *Water Research* **40** (1), 119–125.

Jeong, Y., Fan, M., Singh, S., Chuang, C. L., Saha, B. & Leeuwen, H. V. 2007 Evaluation of iron oxide and aluminum oxide as potential arsenic(V) adsorbents. *Chemical Engineering and Processing: Process Intensification* **46** (10), 1030–1039.

Jones, A. G. 2002 *Crystallization Process Systems*. University College London, UK.

Katsoyiannis, I. A. & Zouboulis, A. I. 2002 Removal of arsenic from contaminated water sources by sorption onto iron-oxide-coated polymeric materials. *Water Research* **36** (20), 5141–5155.

Maiti, A., DasGupta, S., Kumar Basu, J. & De, S. 2007 Adsorption of arsenite using natural laterite as adsorbent. *Journal of Separation and Purification Technology* **55** (3), 350–359.

Mandal, B. K. & Suzuki, K. T. 2002 Arsenic round the world: a review. *Talanta* **58** (1), 201–235.

Mohan, D. & Pittman Jr, C. U. 2007 Arsenic removal from water/wastewater using adsorbents-a critical review. *Journal of Hazardous Materials* **142** (1–2), 1–53.

Samarghandi, M. R., Hadi, M., Moayedi, S. & Barjasteh Askari, F. 2009 Two-parameter isotherms of methyl orange sorption by pinecone derived activated carbon. *Iranian Journal Environmental Health Science Engineering* **6** (4), 285–294.

Sarkar, S., Blaney, L. M., Gupta, A., Ghosh, D. & SenGupta, A. K. 2008 Arsenic removal from groundwater and its safe containment in a rural environment: validation of a sustainable approach. *Environmental Science & Technology* **42** (12), 4268–4273.

Shih, Y., Huang, R. & Huang, Y. 2015 Adsorptive removal of arsenic using a novel akhtenskite coated waste goethite. *Journal of Cleaner Production* **87** (1), 897–905.

Smedley, P. L. & Kinniburgh, D. G. 2001 Source and behavior of arsenic in natural waters. In: *United Nations Synthesis Report on Arsenic in Drinking Water British Geological*

Survey. United Nations, New York. http://www.bvsde.paho.org/bvsacd/who/arsin.pdf.

Tavolaro, A. & Drioli, E. 1999 Zeolite membranes. *Advanced Material* **11** (12), 975–996.

Treacy, M. M. & Higgins, J. B. 1996 *Collection of Simulated XRD Powder Patterns for Zeolites*. 5th edn, Elsevier, New York, p. 586.

Vergili, I., Soltobaeva, G., Kaya, Y., Beril Gonder, Z., Cavus, S. & Gurdag, G. 2013 Study of the removal of Pb(II) using a weak acidic cation resin: kinetics, thermo dynamics, equilibrium, and breakthrough curves. *Journal of Industrial & Engineering Chemistry Research* **52** (26), 9227–9238.

Yan, T., Jiang, S., Zhang, H. & Zhang, X. 2015 Preparation of novel Fe-ZSM-5 zeolite membrane catalysts for catalytic wet peroxide oxidation of phenol in a membrane reactor. *Chemical Engineering Journal* **259**, 243–251.

Zazo, J. A., Fraile, A. F., Rey, A., Bahamonde, A., Casas, J. A. & Rodriguez, J. J. 2009 Optimizing calcination temperature of Fe/activated carbon catalysts for CWPO. *Journal of Catalysis Today* **143** (3–4), 341–346.

Zhou, L., Wang, Y., Liua, Z. & Huang, Q. 2009 Characteristics of equilibrium, kinetics studies for adsorption of Hg(II), Cu(II), and Ni(II) ions by thiourea-modified magnetic chitosan microspheres. *Journal of Hazardous Materials* **161** (2–3), 995–1002.

First received 29 January 2016; accepted in revised form 6 June 2016. Available online 21 June 2016